Journal of
Polymer & Composites

ISSN: 2321-2810 (Online)
ISSN: 2321-8525 (Print)
Volume 13, Regular Issue 5, 2025
DOI (Journal): 10.37591/JoPC

https://journals.stmjournals.com/jopc/

Research JoPC

Effect of 3D Printing Process Parameters on the Tensile Strength of Polylactic Acid (PLA)

Aniket Kolekar [1,]*, Amol Mali[2], Ganesh Jadhav[3], Sunil Dambhare[4], Sandesh Solepatil[5] ,Vikas Dive[6], Rita Kakade[7]

Abstract

This study employs the Taguchi approach to systematically analyze and optimize critical Fused Deposition Modeling (FDM) parameters, focusing on their effect on the tensile strength of 3D-printed Polylactic Acid (PLA) components. The study explores three levels of layer thickness (0.15 mm, 0.25 mm, and 0.3 mm), infill densities (25%, 50%, and 75%), and nozzle temperatures (200°C, 205°C, and 210°C) across three infill patterns: Triangular, Gyroid, and Zig-zag. A total of nine experimental runs were conducted using the L9 orthogonal array design of experiments (DOE), and the mechanical performance was evaluated through tensile testing in accordance with ISO 527 standards. The findings revealed that infill density had the greatest impact on tensile strength, with layer thickness and nozzle temperature being the next most significant parameters. Among the tested patterns, the triangular infill yielded the highest tensile strength of 45.03 MPa at 75% infill density, 0.15 mm layer thickness, and 210°C nozzle temperature. The tensile performance was validated using COMSOL Multiphysics finite element simulations, showing close agreement with experimental results. Statistical analysis using MINITAB-18 and ANOVA confirmed the significance of the parameters. This comprehensive study not only identifies optimal parameter combinations for PLA-based 3D printing but also provides valuable insights for improving the structural performance of FDM components in engineering applications.

Keywords: 3D Printing, polylactic acid (PLA), MINITAB-18 ANOVA, taguchi method, tensile strength

INTRODUCTION

Additive manufacturing, commonly referred to as 3D printing, is a process where objects are built layer by layer from a digital design. This technique involves the sequential deposition of materials such as plastic, metal, or resin to create the desired three-dimensional object. Various 3D printing methods exist, including Stereolithography (SLA), Selective Laser Sintering (SLS), Fused Deposition Modeling (FDM), Digital Light Processing (DLP), Multi Jet Fusion (MJF), PolyJet, Direct Metal Laser Sintering (DMLS), and Electron Beam Melting (EBM) [1]. An FDM 3D printer constructs objects by depositing melted filament material onto a build platform, incrementally adding layers. It reads digital design files and translates them into precise movement and material deposition instructions. Once the heated nozzle attains the desired temperature, the machine guides the filament through an extrusion head, where it melts while being conveyed. This movable head travels along the X, Y, and Z axes, precisely depositing thin strands of molten material layer by layer, following the programmed path from the design file. Fans on the extrusion head can sometimes accelerate the cooling and solidification process [2,3].

***Author for Correspondence**
Aniket Kolekar
E-mail: aniket.kolekar@dypiu.ac.in

[1,3]Associate Professor, Department of Mechanical Engineering, D Y Patil International University, Akurdi, Pune, Maharashtra, India
[2,5,6]Assistant Professor, Department of Mechanical Engineering, D Y Patil International University, Akurdi, Pune, Maharashtra, India
[4]Professor, Department of Mechanical Engineering, D Y Patil International University, Akurdi, Pune, Maharashtra, India
[7]Assistant Professor, ASM Institute of Business Management and Research, Chinchwad, Pune, Maharashtra, India

Received Date: June 11, 2025
Accepted Date: July 01, 2025
Published Date: July 29, 2025

Citation: Aniket Kolekar, Amol Mali, Ganesh Jadhav, Sunil Dambhare, Sandesh Solepatil, Vikas Dive, Rita Kakade. Effect of 3D Printing Process Parameters on the Tensile Strength of Polylactic Acid (PLA). Journal of Polymer & Composites. 2025; 13(5): 128–140p.

P. Chennakesava and Y. Shivraj Narayan explored the complexities of Fused Deposition Modeling (FDM) in additive manufacturing [4]. Kaptan, A., and Kartal, F. identified key FDM route parameters impacting the quality of fabricated parts, aiming to analyze their effects on various performance metrics and compare methods for optimizing FDM process parameters [5]. Gonzalez, Y. E., et al. examined how print speed, layer thickness, and infill density influence the crafting period, using Taguchi and ANOVA methods to minimize lead time in FDM part production. Their findings indicated that infill density and layer thickness significantly affect the crafting period, with layer thickness being the most critical factor [6]. A. E. Tontowi et al. studied tensile strength and dimensional error in 3D printing, focusing on layer thickness, nozzle temperature, and raster angle (RA) for PLA material using Taguchi and Response Surface Methods (RSM). Optimal parameter settings from RSM and Taguchi outperformed manufacturer defaults, with RSM providing superior tensile strength and dimensional error predictions. Tensile strength was mainly influenced by layer thickness, while raster angle affected dimensional error [7]. Tymrak et al. investigated the tensile strength and modulus elasticity of PLA and ABS parts produced by four RepRap 3D printers, highlighting the impact of printing parameters on these materials using ASTM D638 standards [8]. M Rismalia et al. examined the relationship between infill pattern and density on PLA material properties, using ASTM D638 tensile tests to determine material qualities. They found that tensile characteristics improved with increased infill density, with the concentric infill pattern yielding the highest tensile values regardless of density, providing a basis for finite element modeling (FEM) [9]. Made Londen Batan et al. assessed the impact of infill rate, pattern, extrusion temperature, and layer thickness on PLA tensile strength, using the Taguchi method with the L9 Orthogonal Array experimental design. Their analysis, based on average and signal-to-noise ratio (SNR) values and ANOVA, identified that a concentric infill pattern at 90% infill rate and 0.2 mm layer thickness produced the optimal tensile strength of 56.876 MPa [10]. Yahir Enrique Gonzalez et al. used a 3x3 factorial design to study shell count, layer height, and infill percentage effects on tensile strength, flexural strength, and printing time for PLA, finding the highest tensile and flexural strength with 90% infill percentage. Their results indicated that shell count and infill percentage most significantly affected mechanical strength, with minimal influence from layer height [11]. Previous research indicates that infill pattern, infill density, layer thickness, and nozzle temperature are key contributors to tensile strength. While many studies focus on the impact of individual parameters, a comprehensive exploration of their combined effects is lacking. This study aims to investigate these combined effects using three distinct PLA layer thicknesses (0.15 mm, 0.25 mm, and 0.3 mm), infill densities (25%, 50%, and 75%), and nozzle temperatures (200°C, 205°C, and 210°C) for three infill patterns (triangular, gyroid, and zig-zag). Each parameter's impact and the optimal combination are statistically assessed, followed by a confirmation experiment to evaluate the optimal parameter combination. This investigation aims to reveal complex relationships and optimize printing settings for superior mechanical properties using tensile testing, MINITAB-18 ANOVA, and COMSOL Multiphysics software 6.0.

MATERIALS AND METHODS

Material and 3D Printer Specification

A biodegradable thermoplastic made from renewable resources is called polylactic acid (PLA) [12]. It usually has good clarity, a melting temperature of 150–160°C, and a glass transition temperature of 55–60°C. Its mechanical properties vary with molecular weight and processing conditions. PLA is environmentally friendly and can be processed using standard methods. PLA material samples are printed using the Snapmaker A350 3D printer. The specs of the Snapmaker A350 3D printer are shown in Table 1.

Design of Experiments by Taguchi Method

This experiment investigates three parameters: layer thickness, extrusion temperature, and infill rate, each with three different levels. The infill patterns tested include triangular, gyroid, and zig-zag, as depicted in Figure 1. The layer thicknesses chosen were 0.15 mm, 0.25 mm, and 0.3 mm, with infill densities of 25%, 50%, and 75%, and nozzle temperatures of 200°C, 205°C, and 210°C. The variance in printing results was analyzed and assessed for tensile strength. Using the Taguchi Orthogonal Array L9 experimental design, as illustrated in Table 2, the optimal set of parameters was identified.

Table 1. Material and specification of Snapmaker A350 3D printer used.

S no.	Properties	Specification
1	Printing Method	Fused Deposition Modeling (FDM)
2	Printer Bed Size	320 x 330 x 350 (mm)
3	Filament Material	Polylactic Acid (PLA)
4	Filament Diameter	1.75 mm
5	Nozzle Diameter	0.4 mm
6	Bed Temperature	80°C
7	Print Speed	50 mm/sec.

Triangular Gyroid Zig-zag

Figure 1. Triangular, Gyroid and Zig-zag infill pattern in three-dimensional printed PLA specimens.

To Calculate the degree of freedom (DOF) for the selection of the Orthogonal Array for Experimentation, the following procedure is used:

- Number of parameters used in 3D printing = 3 (i.e., Infill density, layer thickness, nozzle temperature)
- Number of levels for each parameter =3 (Each parameter has three different levels)
- Total Degree of Freedom (DOF) for 3 parameters = Number of parameters x (Number of parameters - 1)

Thus,

- Total DOF for 3 parameters = 3 x (3-1) = 6
- Minimum No. of experiments = Total Degree of Freedom for parameter + 1 Thus,
- Minimum No. of Experiments = 6+1 = 7

The given statement indicates that a minimum of seven experiments are needed. The number of rows in the orthogonal array equals the number of experiment conditions, and this number needs to match or exceed the degree of freedom [13]. Consequently, there are six degrees of freedom. As a result, L9 is the next orthogonal array that can be used; it is chosen and displayed in Table 2.

Table 2. Taguchi orthogonal array design -L9.

Exp. no.	Control factors		
	Infill density (%)	Layer thickness (mm)	Nozzle temperature (°C)
1	25	0.15	200
2	25	0.25	205
3	25	0.30	210
4	50	0.15	205
5	50	0.25	210
6	50	0.30	200
7	75	0.15	210
8	75	0.25	200
9	75	0.30	205

Specimen Fabrication

The specimens were created and tested to ensure compatibility with the ISO-527 Type IV standard for tensile strength, as shown in Figure 2 [14]. Three-dimensional printing utilizes design simulations generated using computer-aided drafting software, such as CATIA V5R21, to generate products. These designed CAD models are then inserted into a slicer software like Snapmaker Luban, where 3D printing settings are adjusted, such as nozzle (extrusion temperature), infill density, layer thickness, and layer patterns. Once all the settings are finalized, the G-code file is produced using the software and imported to a drive. This G-code file is necessary for the 3D printer to execute the required actions to generate the product geometry.

Tensile Test

The testing of PLA specimens created for the Tensile test was carried out using a Universal Testing Machine (UTM) at Auto Cluster Research and Development Institute, Pimpri, Pune. Test Conditions: Temperature = 24°C, Humidity = 54% RH, extension range = 500 mm, and load range = 5000 N were maintained while conducting the test. The specimens are tested using ISO 527 standards. Figure 3 shows Tinius Olsen UTM for polymers. 3D-printed tensile specimens of PLA material before and after tensile testing are depicted in Figure 4.

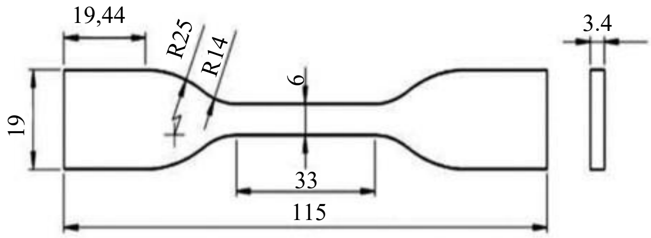

Figure 2. Tensile test specimen as per ISO 527 standards.

Figure 3. Universal testing machine.

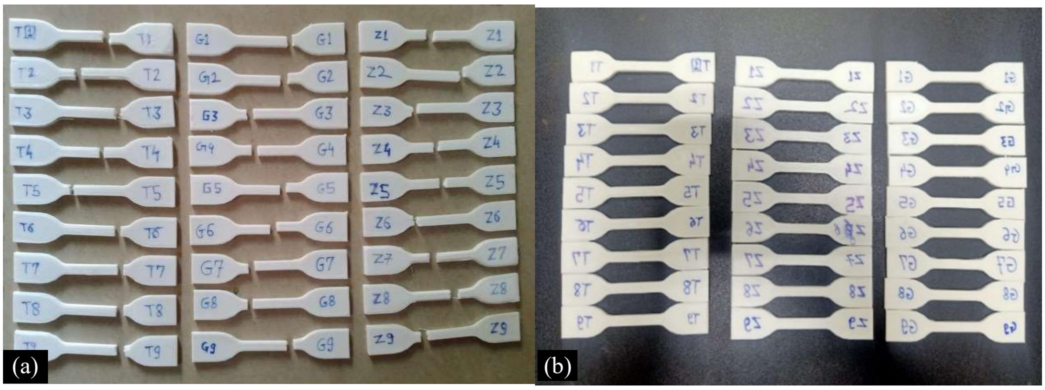

Figure 4. 3D printed tensile test specimens before and after the test (a) After tensile test (b) Before tensile test.

Finite Element Model for Tensile Test

Using the commercial finite element model COMSOL Multiphysics 6.0, a numerical analysis of tensile test specimen was carried out. The static structural analysis of tensile test specimens are simulated by using COMSOL Multiphysics 6.0 software. The von Mises stress analysis was studied at direct load application cases. Because of the software's adaptable features, multiphysics phenomena might be included, allowing a thorough depiction of the intricate material dynamics.

RESULTS AND DISCUSSIONS

Tensile Test Results for Triangular Pattern

This study focuses on maximizing the tensile strength values based on improved printing process parameters. The findings of the specimen's tensile testing in nine printing product studies can be viewed using the experimental design displayed in Table 2. With a 75% infill density, 0.15 mm layer thickness, and 210°C nozzle temperature, experiment number 7 produced a superior tensile strength of 45.03 N/mm² for the triangle pattern. More tensile strength is typically correlated with a higher infill density. The print has enough material at 75% to withstand tensile forces and offer structural support, which minimizes the possibility of interior cavities and weak spots. Better adhesion between layers is made possible by reduced layer thickness. Because the layers adhere to one another more firmly and are less likely to delaminate under stress, this enhances the print's overall integrity. A greater interlayer adhesion is achieved by printing PLA at 210°C, which guarantees that the PLA is sufficiently heated to flow and connect correctly. To prevent problems like weak layer bonding and under-extrusion, proper temperature management is essential.

Table 3. Tensile test results for triangular pattern.

Exp no.	Control factors			Tensile strength(N/mm^2)	Printing time (minutes)
	Infill density (%)	*Layer thickness (mm)*	*Nozzle temperature (°C)*	*Triangular*	
1	25	0.15	200	40.31	55
2	25	0.25	205	37.84	35
3	25	0.3	210	35.76	30
4	50	0.15	205	42.96	46
5	50	0.25	210	39.10	42
6	50	0.3	200	41.42	38
7	75	0.15	210	45.03	48
8	75	0.25	200	42.86	43
9	75	0.3	205	42.14	41

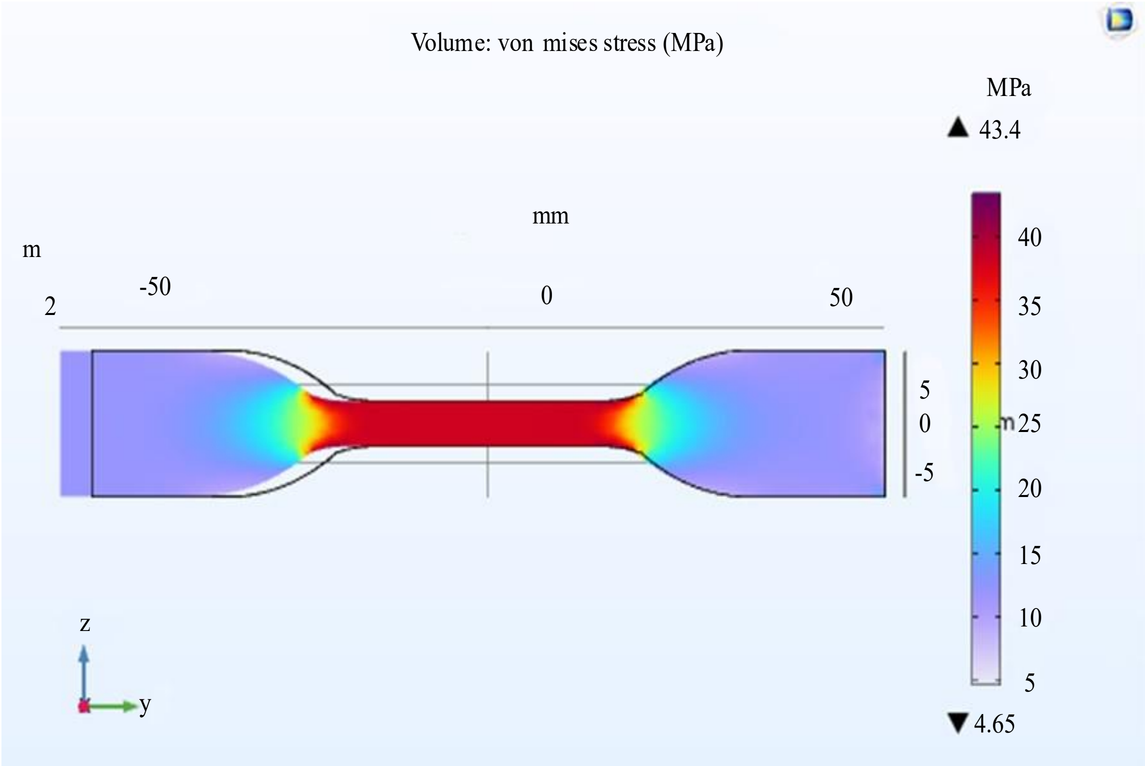

Figure 5. FEA simulation results of tensile test triangular pattern.

The von Mises stress (σ_v) distribution within the tensile test sample corresponds to the circumstance where the counter body slides directly into this sample cross-sectional area during the pull type of loading, as depicted in Figure 5. The maximum tensile strength i.e. 43.4 MPa is observed numerically for 75% infill density, 0.15 mm layer thickness, and 210°C nozzle temperature in a triangular pattern. During the validation of experimental results with the numerical results of the tensile test, a 3.61% variation is observed.

Regression Equation

The following equation (1) shows the regression equation obtained from MINITAB 18 software based on experimental data listed in Table 3. This equation assists in predicting the value of tensile strength for various values of input parameters by illustrating the link between input and output parameters.

Tensile Strength = 72.5 + 0.1075 * Infill Density - 21.15 * Layer Thickness - 0.1567 * Nozzle Temperature (1)

Analysis of Variance

Table 3 shows the analysis of variance (ANOVA) results for the tensile test experimental data, obtained using the general linear model. This analysis, performed with MINITAB software, is detailed in Table 4. The null hypothesis posits that there is no significant difference between the group means under comparison. Variance analysis determines whether to accept or reject the null hypothesis based on a predetermined significance level, which acts as a critical threshold for evaluating the statistical test results. If the calculated p-value, representing the probability of obtaining observed or more extreme results assuming the null hypothesis is true, is less than the significance level, the null hypothesis is rejected. Conversely, if the p-value exceeds the cutoff, the null hypothesis cannot be rejected [13]. The analysis, using a significance level of 0.005, indicates that infill density has a p-value of 0.001, which is below the significance level, leading to the conclusion that infill density significantly impacts tensile strength.

Table 4. ANOVA of triangular pattern.

Source	DF	Adj SS.	Adj MS	F-value	P-value
Regression	3	62.651	20.8835	28.85	0.001
Infill density (%)	1	43.309	43.3091	59.83	0.001
Layer thickness (mm)	1	15.660	15.6598	21.63	0.006
Nozzle temperature (°C)	1	3.682	3.6817	5.09	0.074
Error	5	3.619	0.7239		
Total	8	66.270			

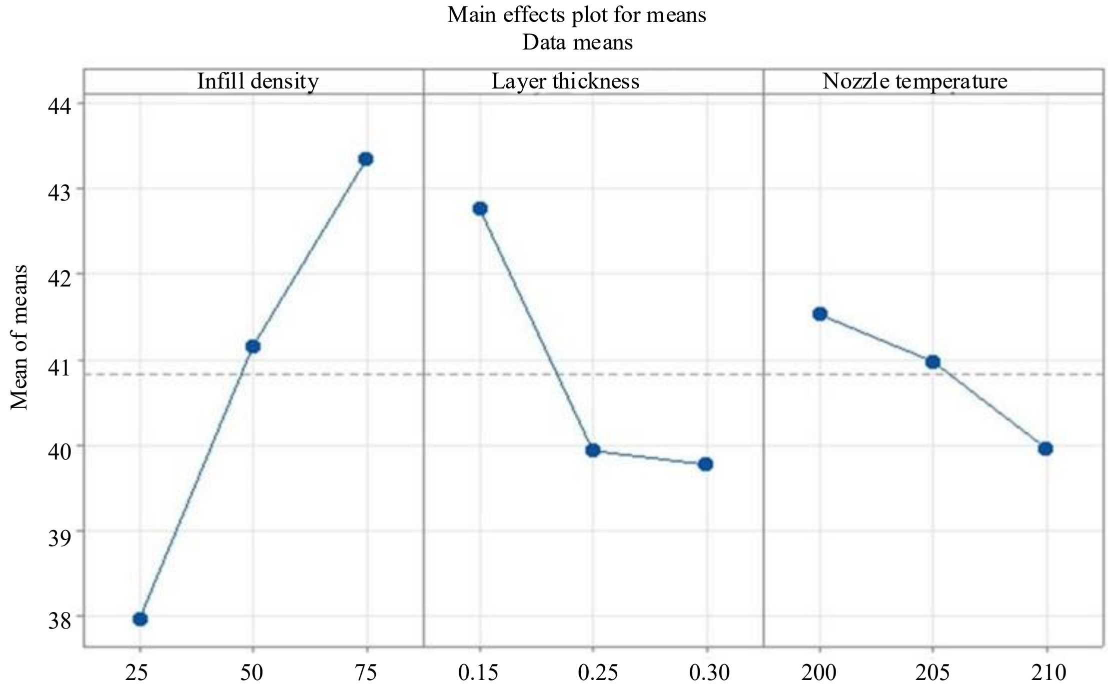

Figure 6. Main effects plot for means of triangular pattern.

Figure 6 illustrates the tensile strength results across different levels. In the case of the triangular pattern, each specimen exhibits varying tensile strengths across the different parameters. It is observed that higher infill densities correspond to increased tensile strength. Conversely, as layer thickness increases, tensile strength tends to decrease. Nozzle temperature shows an inverse relationship with tensile strength. Signal-to-noise ratio analysis was employed to determine the optimal values for each parameter based on the processed data.

The main effect plot and Table 5 shows that the infill density significantly impacts the FDM-printed PLA specimens signal-to-noise (SN) ratio and mean tensile strength. The 75% infill density exhibits the highest SN ratio and mean tensile strength among the three investigated densities. This indicates that the 75% infill density leads to more consistent and more substantial printed parts than 25% and 50% infill densities.

Table 5. Response table for signal-to-noise ratios of triangular pattern.

Level	Infill density (%)	Layer thickness(mm)	Nozzle temperature
1	30.44	30.47	31.03
2	31.17	31.30	31.29
3	32.10	31.95	31.40
Delta	1.66	1.48	0.37
Rank	1	2	3

Tensile Test Results for Gyroid Pattern

This research aims to enhance tensile strength by optimizing the printing process parameters. Table 6 displays the experimental design, showcasing the results from tensile tests conducted on nine printed specimens. Specifically, for the Gyroid pattern, experiment number 9 achieved a superior tensile strength of 43.11 N/mm² using an infill density of 75%, a layer thickness of 0.3 mm, and a nozzle temperature of 205°C.

The von Mises stress (σ_v) distribution within the tensile test sample corresponds to the circumstance where the counter body slides directly into this sample cross-sectional area during the pull type of loading, as depicted in Figure 7. The maximum tensile strength i.e. 44.8 MPa is observed numerically for 75% infill density, 0.3 mm layer thickness, and 205°C nozzle temperature in a gyroid pattern. During the validation of experimental results with the numerical results of the tensile test, a 3.92% variation is observed.

Table 6. Tensile Test Results for Gyroid Pattern.

Exp no.	Control factors			Tensile strength(N/mm²)	Printing time minutes)
	Infill density (%)	*Layer thickness (mm)*	*Nozzle temperature (°C)*	*Gyroid*	
1	25	0.15	200	29.18	40
2	25	0.25	205	33.70	30
3	25	0.3	210	37.49	29
4	50	0.15	205	33.96	39
5	50	0.25	210	36.41	36
6	50	0.3	200	38.34	32
7	75	0.15	210	37.53	69
8	75	0.25	200	40.36	38
9	75	0.3	205	43.11	36

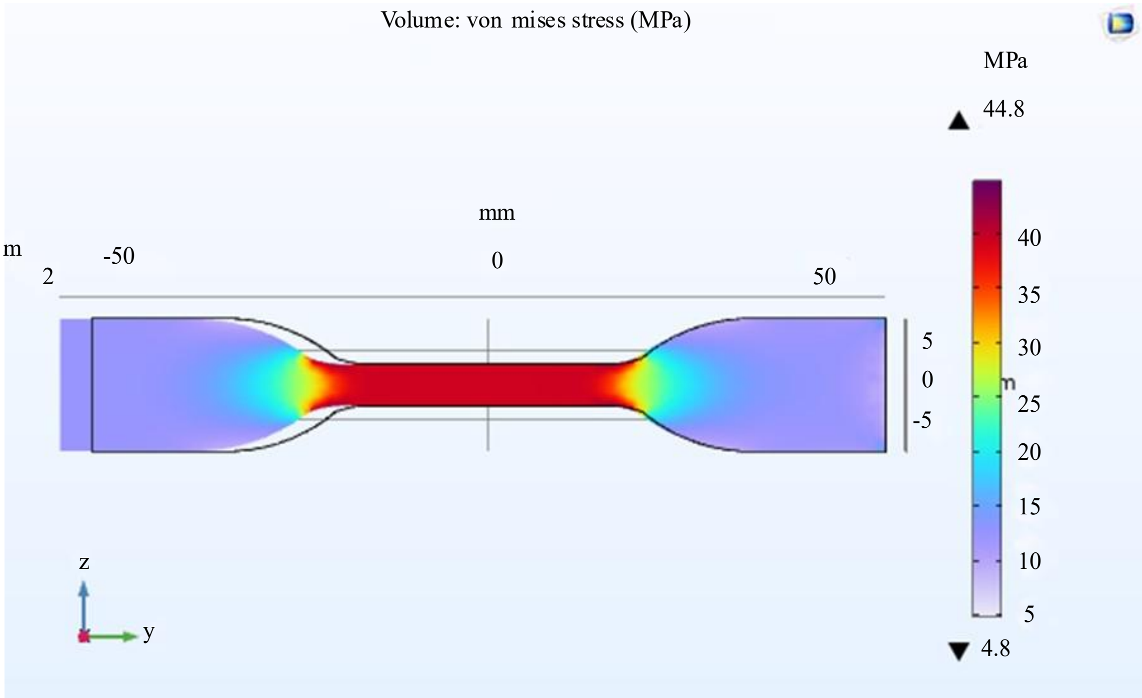

Figure 7. FEA simulation results of tensile test gyroid pattern.

Table 7. Analysis of Variance for gyroid pattern.

Source	DF	Adj SS.	Adj MS	F-value	P-value
Regression	3	127.550	42.5166	52.19	0.000
Infill density (%)	1	70.933	70.9328	87.07	0.000
Layer thickness(mm)	1	54.517	54.5166	66.92	0.000
Nozzle temperature	1	2.100	2.1004	2.58	0.169
Error	5	4.073	0.8146		
Total	8	131.623			

Regression Equation

Equation (2) shows the regression equation obtained from MINITAB software based on experimental data listed in Table 7. This equation demonstrates that the correlation between input and output factors helps predict the value of tensile strength for different input parameter values.

$$\text{Tensile Strength} = -3.7 + 0.1375 * \text{Infill Density} + 39.47 * \text{Layer Thickness} + 0.1183 * \text{Nozzle Temp} \quad (2)$$

The tensile strength results for each level are shown in Figure 8. For the Gyroid pattern, each specimen in each variation has a different tensile strength. The infill density and layer thickness increase in tandem with the tensile strength. Tensile strength is also directly related to nozzle temperature. To find out the optimal value for each parameter, the collected data is then processed using an analysis of the signal-to-noise ratio, as shown in Table 8.

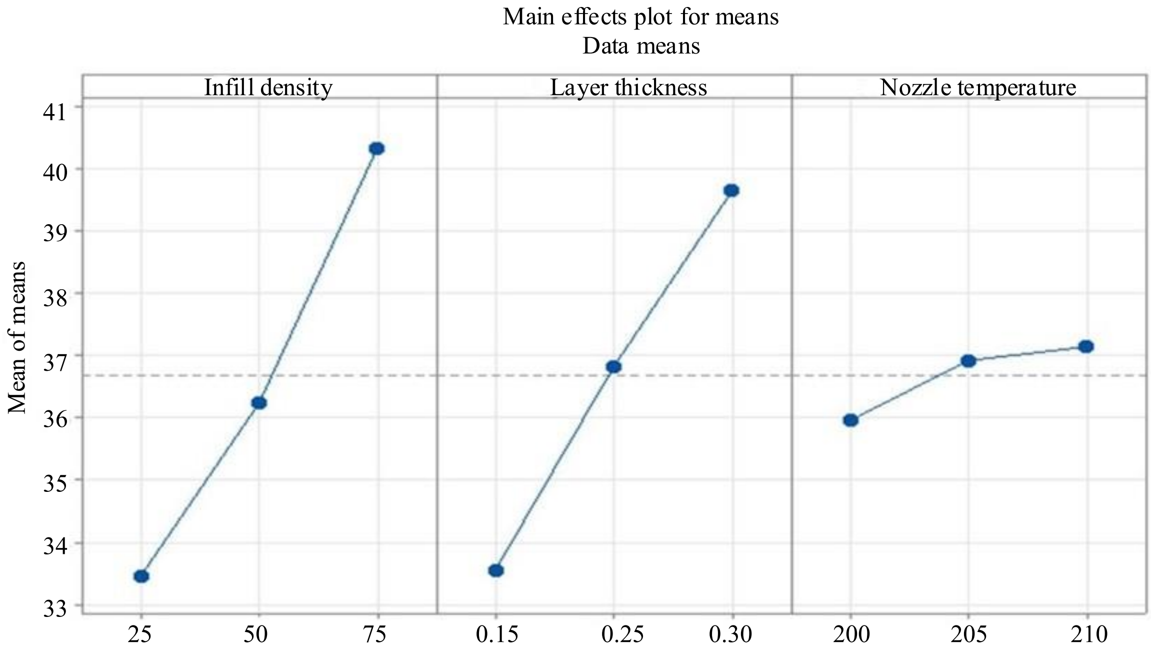

Figure 8. Main effect plot for means of gyroid pattern.

Table 8. Response Table for Signal-to-Noise Ratio of gyroid pattern.

Level	Infill density (%)	Layer thickness(mm)	Nozzle temperature
1	30.44	30.47	31.03
2	31.17	31.30	31.29
3	32.10	31.95	31.40
Delta	1.66	1.48	0.37
Rank	1	2	3

Figure 8 illustrates the tensile strength results across different levels. In the case of the Gyroid pattern, each specimen exhibits varying tensile strengths across different conditions. It is observed that both infill density and layer thickness increase proportionally with tensile strength. Additionally, nozzle temperature shows a direct correlation with tensile strength. The data collected is subsequently analyzed using a signal-to-noise ratio analysis to determine the optimal values for each parameter.

Tensile Test Results for Zig-Zag Pattern

This study focuses on optimizing the tensile strength values based on optimized printing process parameters. The specimens' tensile testing findings in nine printing product studies may be seen with the experimental setup displayed in Table 9. Experiment number 1 produced a higher tensile strength of 43.83 N/mm² for the Zig-zag pattern with an infill density of 25%, layer thickness of 0.15 mm, and nozzle temperature of 200°C.

The von Mises stress (σ_v) distribution within the tensile test sample corresponds to the circumstance where the counter body slides directly into this sample cross-sectional area during the pull type of loading, as depicted in Figure 9. The maximum tensile strength i.e. 44.5 MPa is observed numerically for infill density of 25%, layer thickness of 0.15 mm, and nozzle temperature of 200°C in a gyroid pattern. During the validation of experimental results with the numerical results of the tensile test, a 1.52% variation is observed.

Regression Equation

Equation (3) shows the regression equation obtained from MINITAB software based on experimental data listed in Table 10. This equation shows the relationship between input parameters, fill density, Layer thickness, Nozzle temperature, and output parameter Tensile strength, which helps to predict the significance of tensile strength for different standards of input parameter.

Tensile Strength = 42.7 - 0.0210 * Infill Density - 38.74 * Layer Thickness + 0.032 * Nozzle Temperature (3)

Table 9. Tensile test results for Zig-Zag pattern.

Exp no.	**Control factors**			**Tensile strength (Mpa)**	**Printing time (minutes)**
	Infill density (%)	***Layer thickness(mm)***	***Nozzle temperature (°C)***	***Zig-Zag (Mpa)***	
1	25	0.15	200	43.83	42
2	25	0.25	205	38.72	35
3	25	0.3	210	38.42	29
4	50	0.15	205	42.82	62
5	50	0.25	210	37.34	35
6	50	0.3	200	34.64	28
7	75	0.15	210	41.56	63
8	75	0.25	200	37.88	65
9	75	0.3	205	38.38	40

Table 10. ANOVA for different Parameters of Zig-Zag pattern.

Source	**DF**	**Adj SS.**	**Adj MS**	**F-value**	**P-value**
Regression	3	54.3330	18.1110	6.85	0.032
Infill Density (%)	1	1.6537	1.6537	0.63	0.465
Layer thickness(mm)	1	52.5224	52.5224	19.87	0.007
Nozzle Temperature	1	0.1568	0.1568	0.06	0.817
Error	5	13.2154	2.6431		
Total	8	67.5484			

Journal of Polymer & Composites
Volume 13, Regular Issue 5
ISSN: 2321-2810 (Online), ISSN: 2321-8525 (Print)

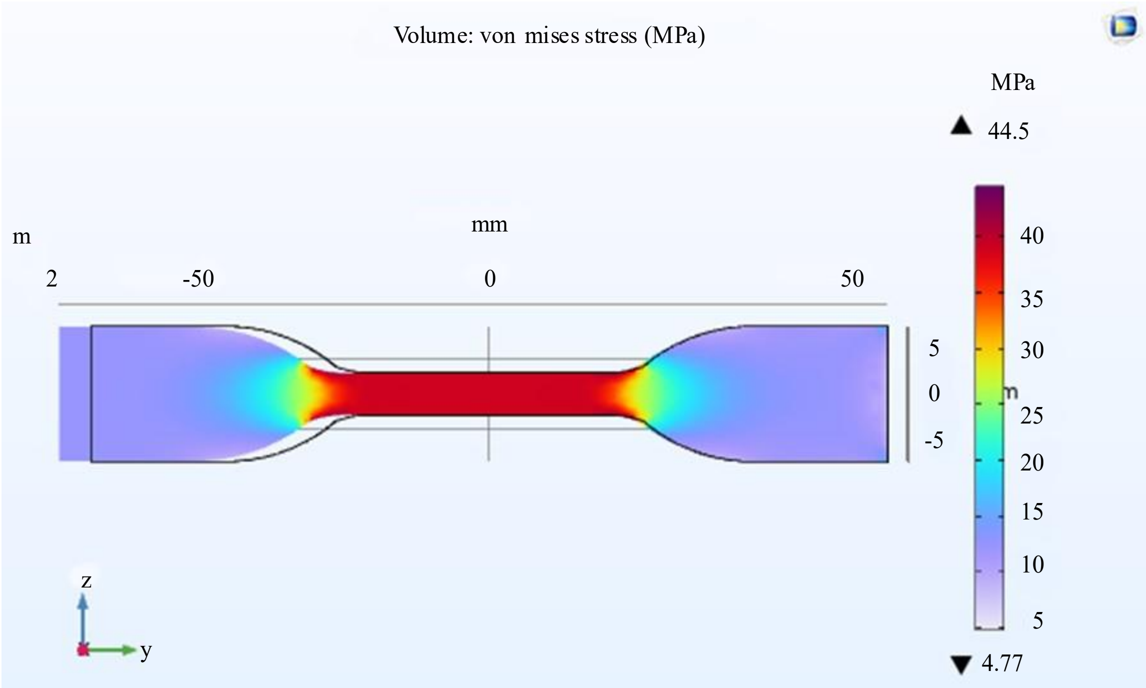

Figure 9. FEA simulation results of tensile test Zig-Zag pattern.

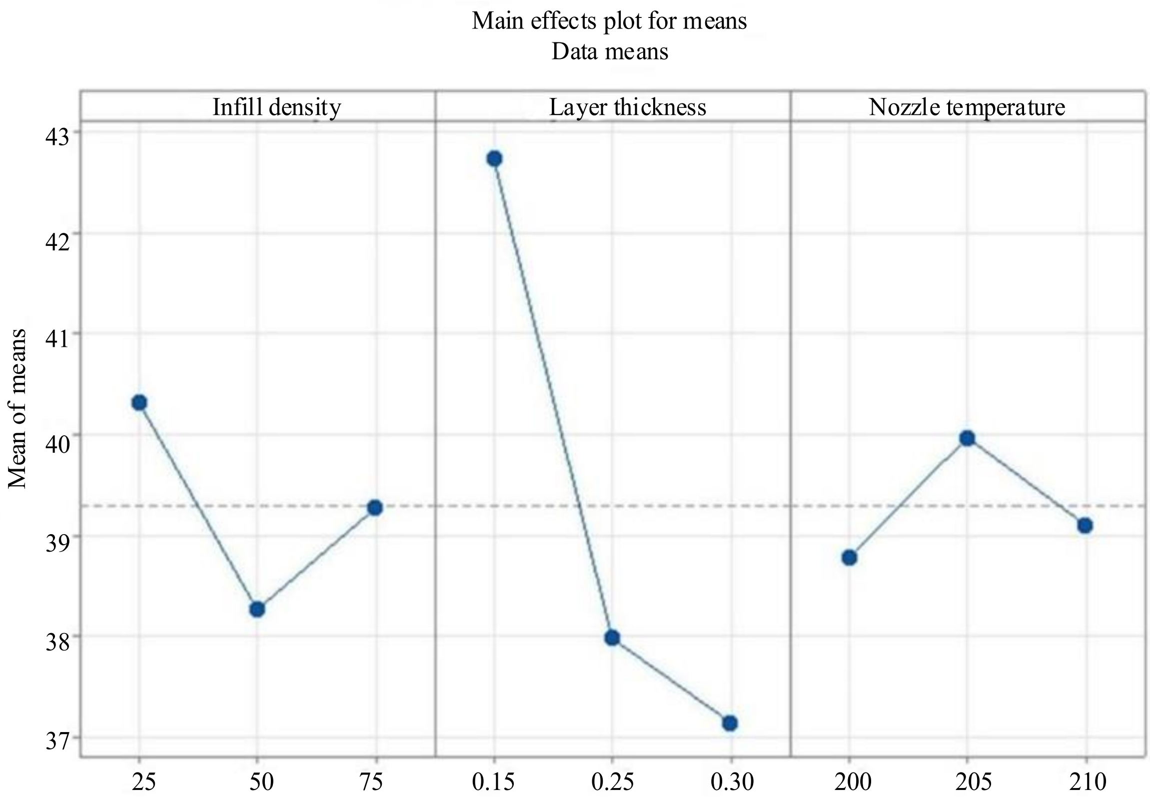

Figure 10. Main effects plot for means of zig-zag pattern.

The graph in Figure10 displays the tensile strength data for each level. It is noted that the tensile strength of each specimen in each version of the Zig-zag pattern varies. The relationship between infill density and tensile strength is inverse. Tensile strength increases with a decrease in layer thickness. Tensile strength is also inversely proportional to nozzle temperature.

Table 11. Response table for Signal to Noise Ratio of Zig-Zag pattern.

Level	Infill density (%)	Layer thickness (mm)	Nozzle temperature
1	32.10	32.61	31.73
2	31.62	31.59	32.02
3	31.87	31.39	31.84
Delta	0.47	1.23	0.29
Rank	2	1	3

Table 12. Tensile strength for all infill patterns.

Exp. no.	Control factors			Tensile strength (N/mm²)		
	Infill density (%)	*Layer thickness(mm)*	*Nozzle temperature*	*Triangular*	*Gyroid*	*Zig-zag*
1	25	0.15	200	40.31	29.18	43.83
2	25	0.25	205	37.84	33.70	38.72
3	25	0.3	210	35.76	37.49	38.42
4	50	0.15	205	42.96	33.96	42.82
5	50	0.25	210	39.10	36.41	37.34
6	50	0.3	200	41.42	38.34	34.64
7	75	0.15	210	45.03	37.53	41.56
8	75	0.25	200	42.86	40.36	37.88
9	75	0.3	205	42.14	43.11	38.38

The obtained data is then analyzed using signal-to-noise ratio analysis to get the ideal value for each parameter as shown in Table 11. The primary effect plot demonstrates that the layer thickness significantly impacts the FDM printed PLA specimens' mean tensile strength and SN ratio. The 0.15 mm layer thickness was investigated, and it was found that it exhibits the highest SN ratio and mean tensile strength among the three levels of layer thickness. This indicates that the 0.15 mm of layer thickness leads to more consistent and more substantial printed parts than other layer thicknesses in case of Zig Zag pattern.

Table 12 shows the tensile strengths of all infill patterns, including triangular, gyroid, and zig-zag. The triangular pattern often provides excellent tensile strength compared to Gyroid and Zig-zag patterns due to its built-in stability and evenly distributed load forces throughout the structure [15]. Gyroid patterns may have other advantages, such as being lightweight and stiff, while Zig-zag patterns are simple but may lack the strength of more complex structures.

CONCLUSIONS

This study focused on the impact of FDM printing parameters on the tensile strength of PLA parts using different infill patterns. The tensile strength increases with higher infill density, with 75% infill density providing the best results across all patterns. Thinner layers (0.15 mm) contribute to higher tensile strength due to better layer adhesion. Higher nozzle temperatures (210°C) generally improve tensile strength by enhancing interlayer bonding. The combination of 75% infill density, 0.15 mm layer thickness, and 210°C nozzle temperature yielded the highest tensile strength (45.03 N/mm²) for the triangular pattern compared to the gyroid and zig-zag. The triangular infill pattern inherently provides a strong geometric structure. Triangles are known for their ability to distribute forces evenly, reducing stress concentrations and enhancing the mechanical properties of the printed object. This makes the triangular pattern more efficient in bearing tensile loads compared to gyroid and zigzag patterns, which may have more complex or less efficient load distribution. This study provides valuable insights for optimizing 3D printing settings to achieve superior mechanical properties in PLA parts.

Acknowledgements

I would like to extend my heartfelt gratitude to Dr. Mrs. A.V. Patil, Director, School of Engineering, Management and Research, Prof. Prabhat Ranjan, Founder Vice Chancellor, D. Y. Patil International University, Pune and Prof. Manish Bhalla, Vice Chancellor, D. Y. Patil International University, Pune for providing the resources and environment that supported this research.

REFERENCES

1. Ali S, Chaurasia DK, Shukla TP. A review: 3D printing. Int J Res Appl Sci Eng Technol. 2022;10(12):1939–41.
2. Jandyal A, Chaturvedi I, Wazir I, Raina A, Haq MIU. 3D printing – A review of processes, materials and applications in Industry 4.0. Sustain Oper Comput. 2022;3:33–42.
3. Siraj I, Bharti PS. 3D printing process: A review of recent research. Sci Prog Res. 2021;1(3):166–76.
4. Chennakesava Sai P, Yeole SN. Fused deposition modeling - insights. In: Proc Int Conf Adv Design Manuf (ICAD&M'14); 2014 Dec 5–7; Tiruchirappalli, Tamil Nadu. p. 1345–50.
5. Kaptan A, Kartal F. The effect of fill rate on mechanical properties of PLA printed samples. Igdir Univ J Inst Sci Technol. 2020;10(3):1919–27.
6. Gonzalez YE, Mendoza JM, Durán JR, Vertel LCT, Rhenals-Julio JD. Effect of printing parameters on mechanical properties and processing time of additively manufactured parts. Matéria (Rio J). 2023;28(3):526–42.
7. Tontowi AE, Ramdani L. Optimization of 3D-printer process parameters for improving quality of polylactic acid printed part. Int J Eng Technol. 2017;9(2):589–600.
8. Tymrak BM, Kreiger M, Pearce JM. Mechanical properties of components fabricated with open-source 3-D printers under realistic environmental conditions. Mater Des. 2014;58:242–6.
9. Rismalia M, Hidajat SC, Permana IGR, Hadisujoto B, Muslimin M, Triawan F. Infill pattern and density effects on the tensile properties of 3D printed PLA material. J Phys Conf Ser. 2019;1402(4):044045.
10. Batan IML, Chandradewi AL, Wahjudi A, Harnany D. Optimization of 3D printing parameter process for product tensile strength from PLA materials using the Taguchi method. JMES Int J Mech Eng Sci. 2023;7(2):90.
11. Gonzalez YE, Mendoza JM, Durán JR, Vertel LCT, Rhenals-Julio JD. Effect of printing parameters on mechanical properties and processing time of additively manufactured parts. Matéria (Rio J). 2023;28(3):1022–34.
12. Bakar AABA, Zainal ABA. Mechanical properties of poly(lactic) acid PLA-based 3D printed filament under temperature and environmental conditions. Mater Today Proc. 2022;67:652–8.
13. Ntumi S. Reporting and interpreting one-way analysis of variance (ANOVA) using a data-driven example: A practical guide for social science researchers. J Res Educ Sci. 2021;12(14):38.
14. Atakok G, Kam M, Koc HB. Tensile, three-point bending and impact strength of 3D printed parts using PLA and recycled PLA filaments: A statistical investigation. J Mater Res Technol. 2022;18:1542–54.
15. Zisopol DG, Minescu M, Iacob DV. Experimental study on mechanical properties of materials used in the oil industry. Eng Technol Appl Sci Res. 2024;14(2):13487–92.

